# COMPILATION OF EARTHQUAKE FAULT PLANE SOLUTIONS IN THE NORTH ATLANTIC AND ARCTIC OCEANS

Páll Einarsson

Science Institute, University of Iceland, 107 Reykjavík, Iceland

Abstract. A set of 95 fault plane solutions for earthquakes along the mid-oceanic ridge system in the North Atlantic and Arctic has been compiled, several of which are reported here for the first time. All the solutions are single event solutions, and most of them are based on teleseismic, long period data. Almost all fault plane solutions for earthquakes in fracture zones show transform faulting, sometimes with a component of reverse faulting. A majority of solutions for earthquakes in the axial zone of the ridges displays normal faulting. P-waves from these earthquakes usually have anomalous radiation pattern; the apparent nodal surfaces are not orthogonal planes. Interference between P, pP and sP is considered to offer the most likely explanation for this phenomenon. Solutions indicating reverse faulting are found near the ridge axis in two areas, near the Bárdarbunga Volcano in Central Iceland, and near 50°N. Volcanic processes such as the deflation of a localized magma chamber may cause this type of faulting, even in the extensional tectonic regime near a divergent plate boundary.

## Introduction

Fault plane solutions of earthquakes play a major part in the theory of plate tectonics. Slip vectors of earthquakes along plate boundaries provide information on the direction of relative motion of the plates on either side, and focal mechanisms of intraplate earthquakes constrain possible models of the driving mechanism of the plates. The implementation of the World Wide Standardized Seismograph Network in the early sixties made available large quantity of high quality long period data with world wide coverage. It then became possible to determine fault plane solutions on a routine basis for most earthquakes larger than magnitude ($m_b$) 5 1/2, even in remote areas such as the mid-oceanic ridges in the Atlantic and arctic Oceans. Since then a multitude of papers have been published describing seismicity and fault plane solutions of major plate boundaries. The present paper grew out of an effort to summarize research on the seismicity along the boundary between the North American and Eurasian plates [Einarsson, 1985] shown in Figure 1. Collecting and editing previously published work on fault plane solutions along this boundary proved to be a nontrivial task. Furthermore, it turned out that substantial amount of data existed that had not been analyzed for fault plane solutions. This report therefore contains fault plane solutions for several earthquakes that have not been studied before, in addition to a compilation of previously reported solutions. It is hoped that the outcome is a relatively homogeneous data base, that can be used in future studies of plate motions and dynamics. The results are given in the Appendix, along with first motion plots of solutions presented in this paper. All solutions are shown schematically on seismicity maps in Figures 2-9.



## Previous Studies

One of the most difficult parts of a compilation work is to select the material to be included. The papers on the subject differ enormously with regard to the methods used, amount of work and thoroughness of documentation, and it becomes inevitable to pass a judgement on the reliability of the published work. Following guidelines were used in the selection:

1. The fault plane solution is based primarily on long-period data, i.e. the wavelength is comparable to the source dimensions. Short period data are often difficult to use and lead to inconsistencies [Stefánsson, 1966; Sykes, 1967].
2. The seismograms should preferentially be read by the author. First motions reported in bulletins are often inconsistent, and turn out to be in error.
3. If the solution is based on P-wave first motion, a plot of the focal sphere should be included, so that the reader may judge the reliability of the solution.
4. Composite fault plane solutions, i.e. where data for more than one event are needed to obtain a solution, are rejected.

If more than one fault plane solution was avail-

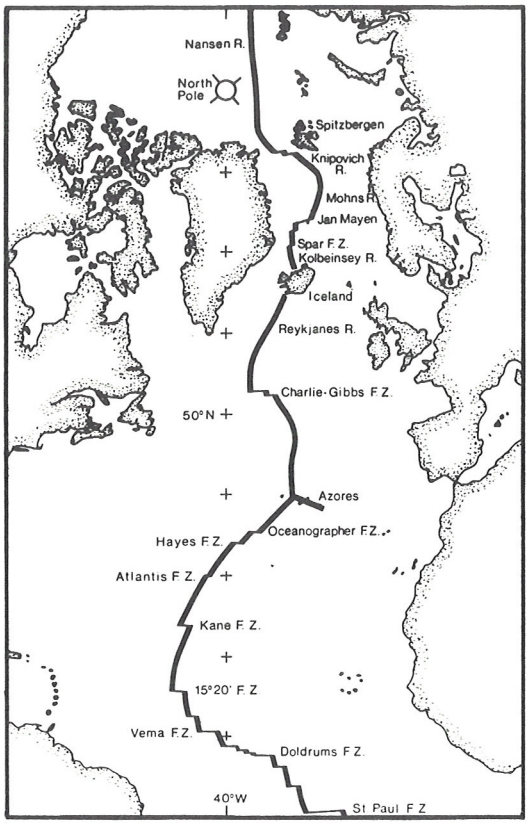


Fig. 1. Index map of the plate boundaries in the North Atlantic and Arctic Oceans.

able for the same event, the one was selected that most closely conformed to the guidelines. Strict use of the criteria excludes all earthquakes before the installation of the WWSSN. If not given in the original publications, poles of nodal planes, P- and T-axis, as well as O-axis of the solutions were derived and tabulated. Small and obvious errors were corrected in a few instances.

During the last few years focal mechanisms based on moment tensor inversion have been published in the Preliminary Determination of Epicenters listings of the U.S. Geological Survey, including several earthquakes in our study area. Awaiting further documentation these mechanisms have been omitted from the present compilation.

## New Solutions

All new fault plane solutions reported here are based primarily on first motions of P-waves. In a few cases S-wave polarization was determined to better constrain the solution. All records were read by the author. First the arrival time of the P-wave was read from the short period record, and then the first motion was determined from the long period record at the appropriate time. By this procedure it is felt that the danger of erroneous picking of the first P-wave excursion is minimized. The rays were projected back to the focal sphere in a standard way using the Herrin tables. The earthquakes were assumed to originate in the lower part of the crust. Focal sphere plots of the new solutions are shown in the Appendix. Data from the WWSSN and Canadian network were used exclusively.

## Non-Orthogonal Nodal Planes

Most authors studying focal mechanisms of mid-oceanic ridge earthquakes have come across the phenomenon that for some earthquakes the dilatational and compressional fields of the focal sphere cannot be separated by two orthogonal planes. This is observed for nearly all earthquakes in the axial zones of the Mid-Atlantic Ridge for which sufficient data are available. In the fracture zones, on the other hand, no examples have been found so far. Several explanations have been suggested for this phenomenon:

1. The apparent nonorthogonality is the result of the bending of rays passing through a low velocity lens beneath the ridge axis [Solomon and Julian, 1974].

2. The anomalous radiation pattern is the effect of near-source anisotropy related to preferred orientation of olivine crystals in the ridge mantle [Kawasaki and Tanimoto, 1981].

3. The earthquake source has an explosive component superimposed on the double couple [Solomon and Julian, 1974].

4. The earthquake occurs by extension failure of a porous, fluid-saturated medium [Robson et al, 1968]. The opening of an extension crack is accompanied by a sudden drop in fluid (magma) pressure. Thus an implosive component is superimposed on the compressive field from the extension crack.

5. The first motion pattern is obscured by the surface reflected phases pP and sP [Hart, 1978; Tréhu et al., 1981]. For a shallow source the arrival time difference between the reflected phases and the direct P-wave may be short compared to the response time of the long period seismographs. This effect would only occur for earthquakes with a significant dip-slip component.

All these suggestions deserve serious attention. The last explanation is favoured here, mainly because of the convincing arguments presented by Tréhu et al. [1981]. They inverted the Rayleigh waves from an event on the Reykjanes Ridge, for which non-orthogonal nodal planes had been found, and derived the moment tensor. The source mechanism turned out to be primarily of the double-couple type. They then calculated synthetic seismograms taking into account the surface reflected phases and the response of the seismographs, that showed remarkable similarity with actual data. The fourth possibility may also deserve special investigation in the light of recent findings of Julian [1983] for the Mammoth Lake events of 1980 associated with renewed activity of the Long Valley Caldera, and Foulger

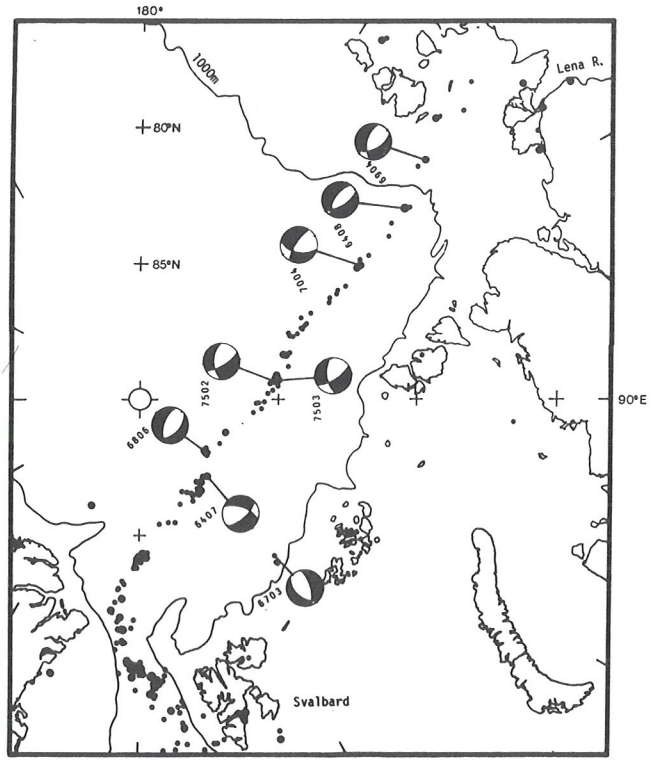


**Fig. 2. Epicenters and fault plane solutions in the Arctic Basin. Epicenters are taken from the PDE lists of USGS for the period 1962-1981, only epicenters determined with 10 or more stations are included. Epicenters of events of $m_b$ = 5.0 and larger are marked with large dots. The fault plane solutions are shown schematically as lower hemisphere stereographic projections of the focal sphere. The compressional quadrants (containing the least compressive stress axis) are shown black. Numbers give year and month of the earthquake.**

[1984] for some earthquakes in the Hengill geothermal area in Iceland. A compensated linear vector dipole (CLVD) model seems to best conform with their data. This corresponds to an extensional crack with a superimposed pressure drop. The projections of the nodal surfaces onto the focal sphere are small circles centered on the T-axis.

Taking away the constraint of orthogonality of nodal planes it becomes impossible to obtain a focal mechanism solution for most earthquakes from first motions of P-waves alone. More sophisticated methods have to be applied. This constitutes a problem in this compilation work. Some of the fault plane solutions of normal faulting earthquakes reported in the literature are obtained with limited data, leaning heavily on the assumption of orthogonal nodal planes. Accepting minor inconsistencies, it is in many cases possible to find orthogonal planes if the station distribution on the focal sphere is uneven. This should be born in mind when reading the fault plane solution maps in Figures 2-9 and the table in the Appendix. In spite of this problem it is in many cases possible to infer the type of faulting and the general attitude of the T-axis from the first motion pattern, even if the exact position of the nodal surfaces cannot be determined.

## The Arctic Plate Boundary

We will now trace the plate boundary from the continental shelf of Siberia near the Lena River delta, across the Arctic Basin, past Svalbard, along the Knipovich and Mohns Ridges, the Jan Mayen Fracture Zone, and the Kolbeinsey Ridge, to Iceland.

On the continental shelf of Siberia, the seismicity of the plate boundary is dispersed over a wide area, probably reflecting the continental lithospheric structure as well as the proximity to the pole of relative plate rotation. This area was noted for its relatively large earthquakes already by Tams [1927]. A fault plane solution by Conant [1972] shows normal faulting with non-orthogonal nodal planes. This is noteworthy because it shows that this phenomenon can occur in continental environment.

As the late boundary crosses the continental shelf edge over to the oceanic structure the seismic belt becomes narrow. It follows the crest of the Nansen (Gäkkel) Ridge for about 2000 km across the Arctic Basin (Figure 2). The ridge is almost straight, uninterrupted by large offset transform faults. The seismicity is moderately high and all available fault plane solutions show normal faulting at the ridge crest [Savostin and Karasik, 1981; Sykes, 1967].

North-east of Greenland the plate boundary makes a turn and follows the Lena Trough southwards to the Spitsbergen Fracture Zone (Figure 3). The Lena Trough appears to be an obliquely spreading boundary, similar to the Knipovich Ridge farther south. No bathymetric or seismological evidence for transform faulting along these boundaries has been found so far. In the Spitsbergen Fracture Zone, on the other hand, the alignment of epicenters,5 fault plane solutions, the occurrence of large earthquakes and bathymetric features are consistent with transform faulting. The short Molloy Ridge connects it to the Molloy Fracture Zone, which has been seismically quiet for the last two decades.

The Svalbard Archipelago stands out on most seismicity maps as an area of high seismicity. Most of the activity is concentrated in two zones in Heer Land and Nordaustlandet although scattered activity is found in other parts of the archipelago [Bungum et al., 1982]. Teleseismic maps, such as Figure 3, show intraplate activity on the continental shelf west of Svalbard, possibly connecting it to the Knipovich plate boundary. The concentrated earthquake zones in Svalbard are elongate in a WNW-ESE direction and a fault plane

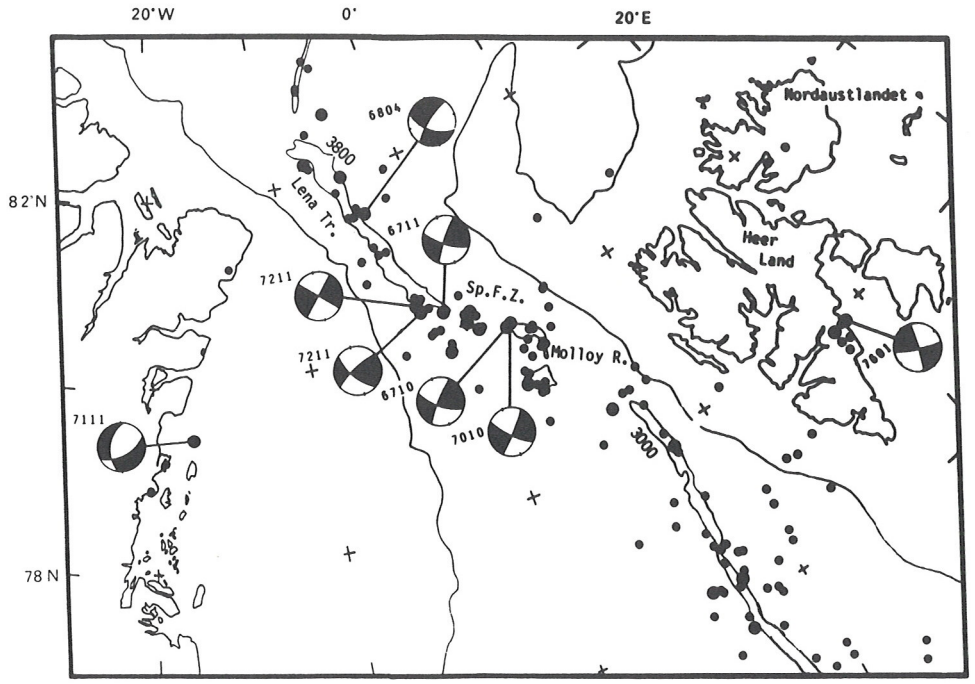


Fig. 3. Epicenters and fault plane solutions in the NE Greenland-Svalbard region. Data and symbols are as in Fig. 2. The continental shelf edge is marked by the 1000 m isobath, rift valleys and depressions associated with the plate boundary along the Nansen Ridge, Lena Trough, Spitsbergen and Molloy Fracture Zones and the Knipovich Ridge are shown with the 3800 and 3000 m isobaths.

solution shows left-lateral strike-slip along this trend. This seismicity was attributed by Bungum et al. [1982] to an interaction between the present tectonic stress field and older zones of weakness. Savostin and Karasik [1981], on the other hand, felt that this seismicity implied the existence of a separate plate, the Spitsbergen microplate, even though its eastern boundary could not be clearly delineated.

The seismicity of the Knipovich Ridge is quite scattered, implying that deformation takes place within a wide zone. This feature is possibly inherited from the time when this part of the plate boundary changed from being primarily of strike slip character to being a divergent boundary, when spreading ceased in the Labrador Sea.

The pattern of seismicity changes abruptly from the Knipovich to the Mohns Ridge. The Mohns Ridge is in most respects a typical mid-ocean ridge, centrally located in the Greenland-Norwegian basin, and uninterrupted by fracture zones of significant offset. The spreading is slightly oblique, especially at its western end, where it joins with the Jan Mayen Fracture Zone at an angle of 120 . The seismic zone is well defined, narrow and continuous along the rifted crest (Figure 4). Fault plane solutions by Conant [1972] and Savostin and Karasik [1981] show normal faulting at the ridge axis.

The Jan Mayen Fracture Zone is the most significant fracture zone in the Arctic region, displacing the ridge axis 210 km to the right. Both ridge-transform intersections are well identified in the topography by the characteristic triangular depressions. The transform section of the fracture zone is a pronounced trough, but highly asymmetric, because of the high topography connected with the Eggvin Bank and the Jan Mayen continental sliver to the south. The overall trend of the transform section is 110°, and all available fault plane solutions are consistent with left-lateral strike-slip along a plane with strike varying between 120° in the east to 102° in the west. This variation hardly justifies much speculation although some authors have felt that an explanation was needed. Bungum and Husebye [1977] suggested that the fracture zone consisted of several en echelon segments striking slightly more E-W than the main zone, and Savostin and Karasik [1981] concluded that the slip vector contained a small component of convergence across the fracture zone. Perhaps a stress concentration around an asperity can explain the variation. The asperity is the island of Jan Mayen that protrudes into the fracture zone about 55 km west of the eastern ridge intersection. The high seismicity of this part of the fracture zone may be an indication of stress concentration.

The plate boundary between Jan Mayen and Iceland follows the Kolbeinsey Ridge, which is

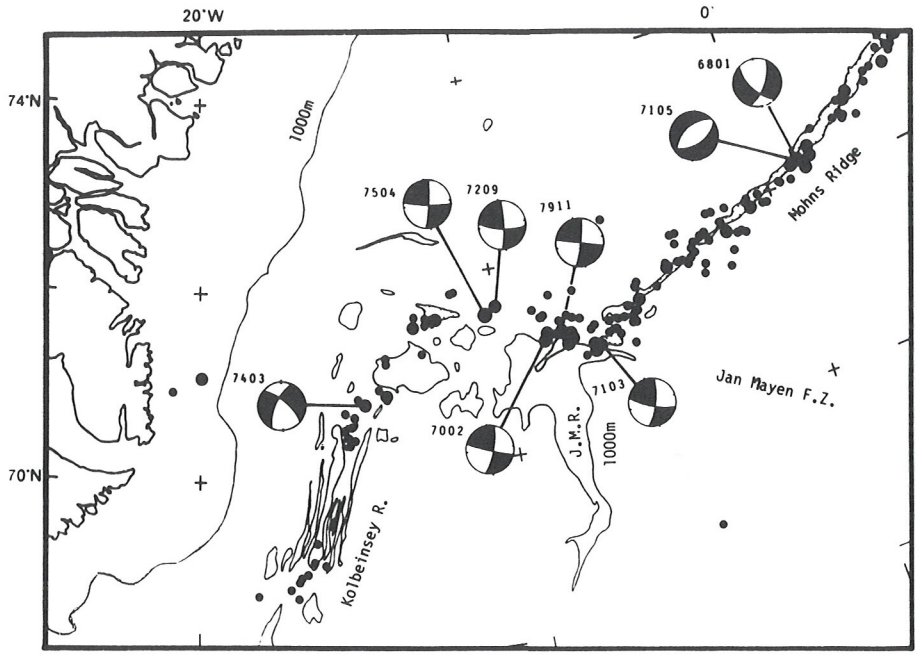


Fig. 4. Epicenters and fault plane solutions in the Jan Mayen area. Data and symbols are as in Fig. 2. The rift valley of the Mohns Ridge and depressions at the ridge-transform intersections are shown by the 2600 m isobath. The 1000 m isobath delineates the Jan Mayen Ridge, Eggvin Bank, and the Kolbeinsey Ridge.

anomalous in several ways. It is asymmetrically located with respect to the adjacent continents, the topography is high and the seismicity low. All these features may be in some way related to the existence of the Iceland hot spot to the south. Two small fracture zones are known on the Kolbeinsey Ridge, one located south of the Eggvin Bank near 71°N, the other near 69°N, the Spar Fracture Zone. These fracture zones are defined by topography and magnetic data, no fault plane solutions are available supporting transform faulting.

## Iceland

Fault plane solutions are available for five areas, i.e. the two transform zones in South and North Iceland, the intraplate Borgarfjordur area in West Iceland, the Bárdarbunga Volcano in Central Iceland and the Katla Volcano in South Iceland (Figure 5). Solutions in the last two areas are reported here for the first time.

The plate boundary is displaced from the Kolbeinsey Ridge eastwards to the neovolcanic zone of Iceland by the Tjörnes Fracture Zone, which is a zone of high seismicity near the north coast of Iceland. The zone has a general E-W trend and fault plane solutions are consistent with transform faulting along the zone. In other respects the zone bears little resemblance to oceanic transform faults. The seismicity is distributed over an 80 km wide zone and is clearly not associated with slip along a single fault. At least three parallel, NW-SE trending seismic belts have been identified, which appear to take up the transform motion at present [Einarsson, 1976, 1979]. The three earthquakes for which fault plane solutions have been obtained did not occur on the same belt. The westernmost event (63 03) probably occurred on the southernmost belt, the Dalvik seismic line, the two other events were associated with the Grímsey seismsic line, which marks the northern boundary of the fracture zone. The easternmost event (76 01) originated at the intersection between the Grímsey line and the Krafla fissure swarm, and was associated with a rifting event along the divergent plate boundary [Björnsson et al., 1977]. It demonstrates the close association between plate separation along a ridge axis and transform faulting on the adjacent transform fault. The sequence of events involved a small basaltic eruption at the Krafla Volcano in the volcanic rift zone, deflation of the volcano, magma migration northwards along the Krafla fissure swarm, accompanied by rifting and large scale horizontal and vertical ground displacements. Transform faulting was initiated when the rifting reached the intersection with the Grimsey line. Activity has continued in the Krafla area since the initial events of December 1975 - January 1976, involving lateral migration of magma, eruptions and rifting.

A cluster of epicenters appears in Central Iceland in Figure 5. Most of this activity is as-

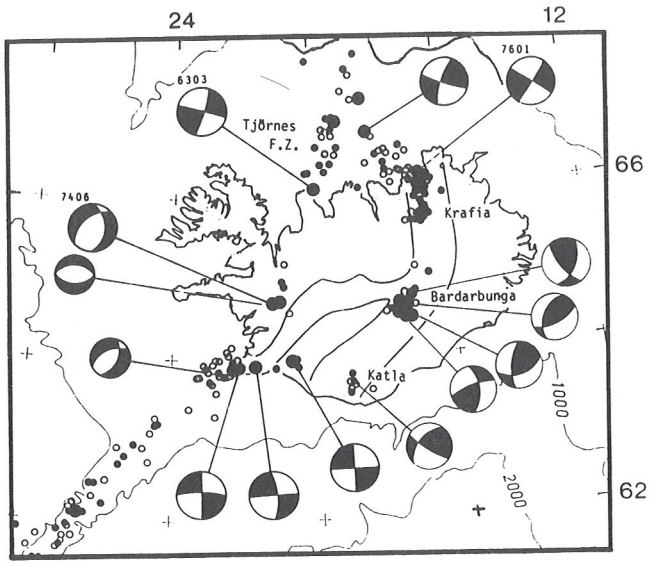


Fig. 5. Epicenters and fault plane solutions in Iceland. Data and symbols are as in Fig. 2.

sociated with the subglacial Bárdarbunga Volcano, which is one of the central volcanoes that characterize the structure of this part of the rift zone. A distinct sequence of earthquakes, with seven shocks reaching magnitude larger than 5 ($m_b$) occurred under Bardarbunga in 1974-1980, but events of that size were unknown there before. Four fault plane solutions have been determined, all showing reverse faulting. This result is somewhat unexpected, especially since Bardarbunga is located in a rift zone near the center of the Iceland hot spot [see e.g. Sigvaldason et al., 1974] where one would usually assume plate divergence and normal faulting. An inflating magma chamber would also cause extension and normal faulting in the crust above. Deflation, on the other hand, would lead to horizontal contraction and reverse faulting in the magma chamber roof. Seen in this perspective the increased seismic activity in 1974-1980 is an indication of decreasing pressure or magma withdrawal from underneath Bardarbunga. It is noteworthy in this context, that the Krafla Volcano in the rift zone about 110 km north of Bardarbunga was inflating during the same period. This may, of course, be coincidental, but it is also possible that some kind of a pressure connection between the volcanoes exists at subcrustal depths. The partially molten layer inferred from seismic and magneto-telluric data [Gebrande el al., 1980; Beblo and Björnsson, 1980] to lie beneath large parts of Iceland at the depth of 10-20 km could act as a conductor of pressure variations between volcanoes.

A group of epicenters is also seen in Figure 5 in the volcanic zone in South Iceland. These earthquakes are associated with the subglacial Katla Volcano, which is situated south of the ridge-transform intersection in South Iceland. One poorly constrained fault plane solution indicates strike-slip with a significant component of reverse faulting. As in the case of Bárdarbunga, a deflating magma chamber may offer an explanation for this type of faulting.

Most of the seismicity in SW-Iceland is attributed to a complex zone of transform faulting that connects the southern part of the volcanic zone to the submarine Reykjanes Ridge. The tectonic characteristics change along this zone, as one goes from the South Iceland seismic zone, that bridges the gap between the two branches of the volcanic zones, to the Reykjanes Peninsula, that displays high volcanic activity as well as high seismicity. Historically the largest earthquakes have occurred in the easternmost part of the zone; the maximum magnitude decreases as one goes westwards. Surface fracturing during historical earthquakes in the South Iceland seismic zone shown that each individual event is associated with right-lateral strike-slip faulting on N-S striking fault planes, in spite of the clear E-W alignment of the epicenters [Einarsson and Eiriksson, 1982; Einarsson et al., 1981]. The only available fault plane solution [Ward, 1971] in this part of the zone is consistent with this type of faulting. Most surface fractures on the Reykjanes Peninsula have a NE-SW trend, arranged en echelon with respect to the seismic zone, and appear to be related to magmatic activity. Two teleseismic fault plane solutions show strike-slip faulting on E-W or N-S striking planes [Ward, 1971; Einarsson, 1979]. Numerous solutions were also determined for small earthquakes by Klein et al., [1973, 1977] using dense, local seismic arrays. The T-axis of the solutions is consistently oriented in a horizontal, NW direction. The P-axis rotates between the vertical direction in normal faulting solutions and the horizontal NE direction in strike-slip solutions. Thus the stress regime is characterized by the NW-trending minimum compressive stress. The other principal stresses are probably nearly equal and may change directions according to local, or time dependent conditions. Dikes and eruptive fissures open up against the minimum stress and strike NE. There is a systematic trend along the peninsula from more strike-slip faulting in the eastern part to more normal faulting in the west, where the seismic zone gradually bends to the SW to join the Reykjanes Ridge.

A sequence of earthquakes occurred in West-Iceland in 1974, well outside the zones of rifting and volcanism normally attributed to the plate boundary. The sequence was studied by Einarsson et al. [1977], who determined a teleseismic fault plane solution for the largest shock, and several single event and composite solutions using data from a dense local array of seismographs. All solutions show normal faulting, indicating horizontal extension in this intraplate region.

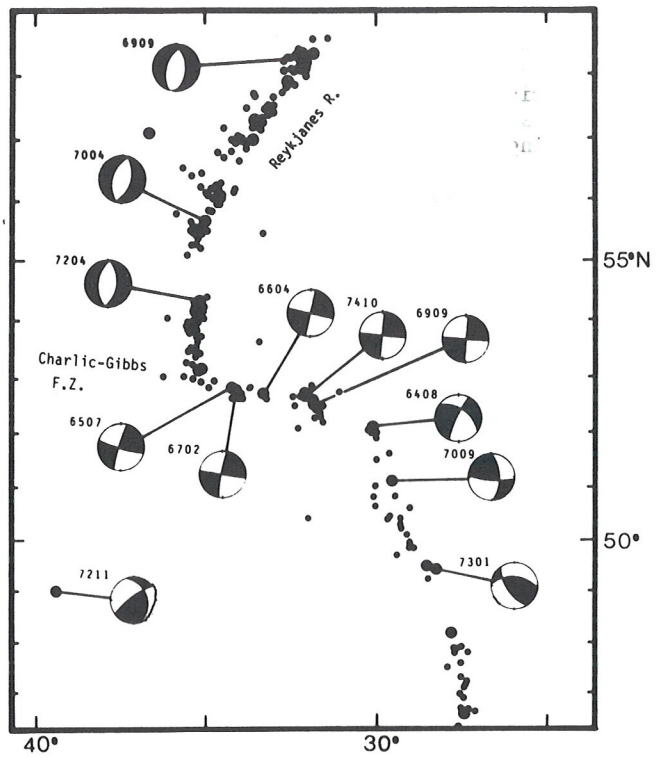


**Fig. 6. Epicenters and fault plane solutions in the Charlie-Gibbs Fracture Zone and along the adjacent ridges. Data and symbols are as in Fig. 2.**

From Iceland to the Azores

This section of the mid-Atlantic plate boundary consists of two gently arcuate ridges, offset near 52°N by a major fracture zone, the Charlie-Gibbs Fracture Zone. Nearest to Iceland the seismicity of the ridge is relatively low. Fault plane solutions have not been obtained for this reason. In this respect the Reykjanes Ridge shows a certain similarity with the Kolbeinsey Ridge north of Iceland. The low seismicity has been ascribed to the proximity to the Iceland hot spot [see e.g. Vogt, 1978]. Farther south the ridge crest gradually turns from a N35°E trend to a more southerly direction, and south of 58 1/2°N the seismicity attains levels comparable to other parts of the ridge. Four fault plane solutions are available all with non-orthogonal nodal planes. Two of them are for events in the same swarm (70 04), and are shown as one in Figure 6.

The Charlie-Gibbs Fracture Zone offsets the ridge crest about 350 km to the left. It consist of two parallel troughs, 45 km apart. A short spreading axis joins the troughs near 31°45'W, so transform faulting takes place in the western part of the northern trough and eastern part of the southern trough . This is confirmed by 5 fault plane solutions for the northern trough, but the southern trough has been seismically quiet for the past 25 years. One fault plane solution near the eastern ridge intersection shows oblique faulting. Oblique structures have been found near some ridge-transform intersections, e.g. the eastern Charlie-Gibbs [Searle, 1981], in the FAMOUS area [Whitmarsh and Laughton, 1975] and the Vema Fracture Zone [Forsyth and Rowlett, 1979].

The ridge segment south of the Charlie-Gibbs Fracture Zone, between 48° and 51°N, appears to have same peculiar features. A fault plane solution of an event near 49.5°N shows reverse faulting, and a second solution near 51 N has a significant component of reverse faulting. The seismic zone has a general trend of NNW, and according to Johnson and Vogt [1973] the structure of the ridge is characterized by alternating N-S trending and oblique spreading axes. The N-S axes are associated with transverse basement ridges, that trend slightly north of the spreading direction on both sides of the plate boundary. This "herringbone" pattern in the topography was interpreted as the result of asthenospheric flow southwards from the Iceland hot spot. The intersection of the transverse ridges with the plate boundary are then viewed as the locus of unusually high production of volcanic material, a central volcano complex, that slowly migrates southwards along the plate boundary, leaving a trail of its products on both plates. Thus the reverse faulting solutions may be put into a volcanic context as was the case with the Bárdarbunga and Katla earthquakes in Iceland. Forcible intrusion of viscous magma at shallow depth can cause thrust faulting in the adjacent region, and the deflation of a magma chamber will cause reverse faulting in the chamber roof.

South of 48°N the ridge is fairly straight and fracture zone offsets are too small to be resolved on the seismicity map (Figure 7). Seismic activity is relatively uniform, both in space and time, and earthquakes larger than $m_b = 5$ are rare. Two poorly constrained fault plane solutions indicate normal faulting.

The Eurasian-African plate boundary is marked by a seismic zone that extends from a triple junction with the Mid-Atlantic Ridge near the Azores to Gibraltar. The characteristics of the activity change as one goes along the zone. It can be divided into three segemnts according to its seismic characteristics. The westernmost segment extends from the junction, through the Azores and to the eastern end of the archipelago. The zone is relatively narrow, comparable to the zone on the Mid-Atlantic Ridge, and follows the ESE trend of the archipelago. Fault plane solutions show that strike-slip is the principal mode of faulting, but the nodal planes only rarely strike parallel to the trend of the zone. The largest earthquake of recent years in this area occurred on Jan. 1, 1980. The fault plane solution is of the strike-slip type (see Appendix), and the aftershock study of Hirn et al. [1980] revealed the NNW striking plane as the fault

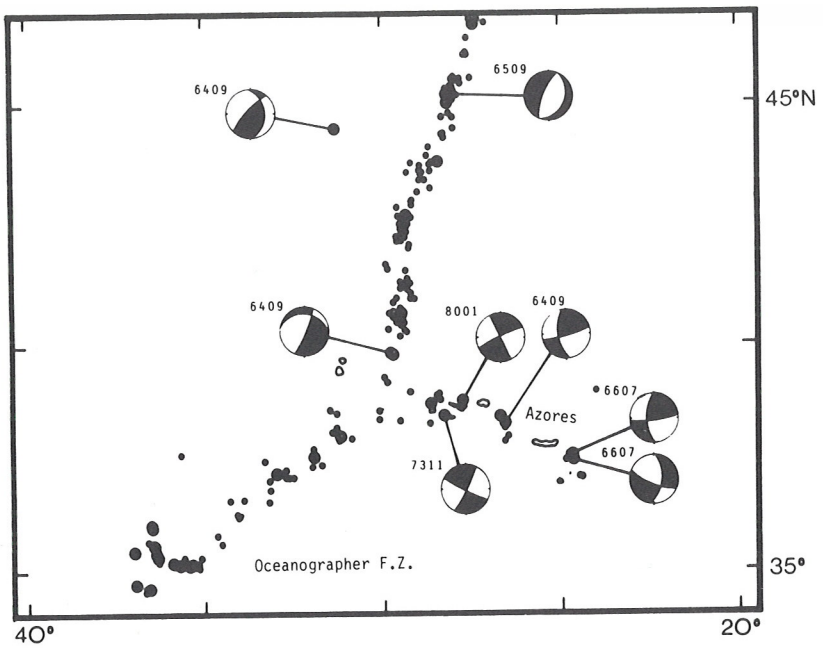


Fig. 7. Epicenters and fault plane solutions near the Azores triple junction. Data and symbols are as in Fig. 2.

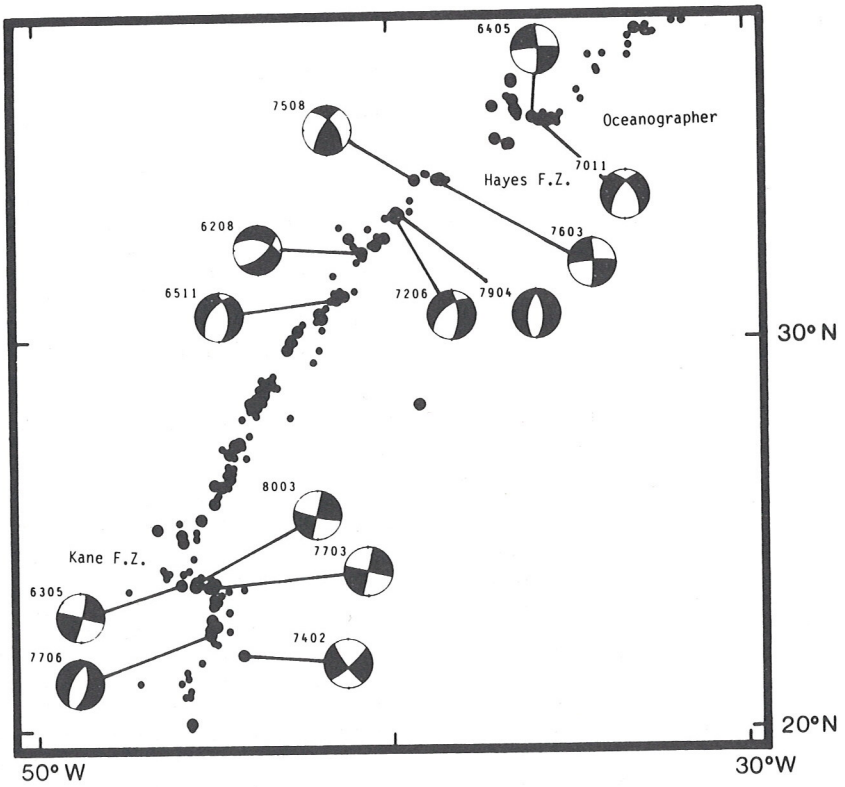


Fig. 8. Epicenters and fault plane solutions along the Mid-Atlantic Ridge between 20° N and 37° N. Data and symbols are as in Fig. 2.

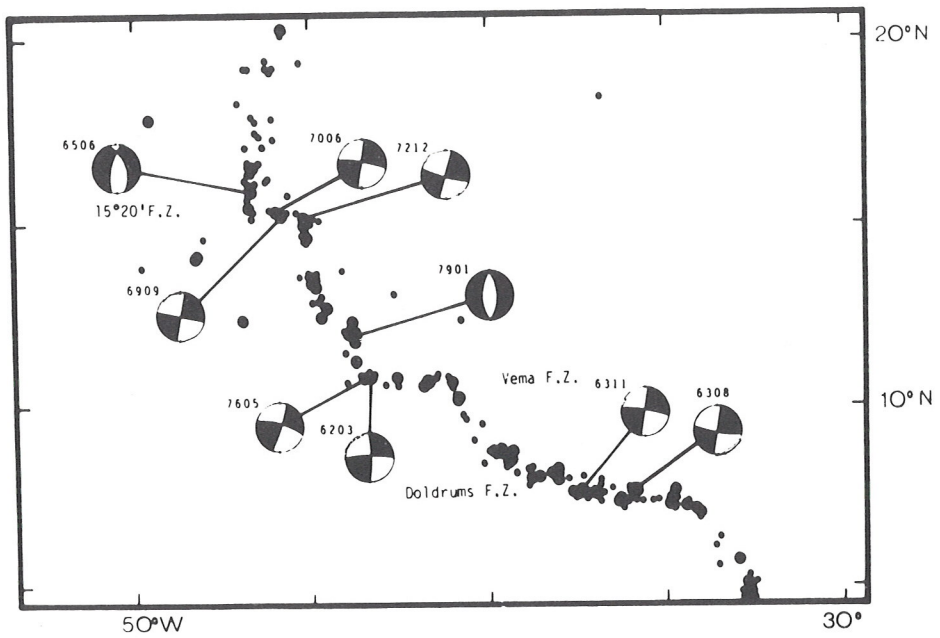


**Fig. 9. Epicenters and fault plane solutions along the Mid-Atlantic Ridge between 5°N and 20°N. Data and symbols are as in Fig. 2.**

plane, thus indicating left-lateral movement. If this result is generalized for the Azores seismic belt, it appears as if the relative plate motion is taken up by a series of en echelon strike-slip faults.

The middle section of the Azores-Gibraltar zone has been seismically quiet for the last decades. East of 18°W the plate boundary is no longer defined by a narrow seismic belt. The high, but diffuse seismicity in this region shows that plate deformation occurs within a 400-500 km wide zone, which extends into the Gulf of Cadiz and is connected to the seismic belt of Morocco and Algiers. Fault plane solutions are characterized by thrust faulting; occasionally strike-slip solutions are seen. A common feature is a maximum compressional axis trending N to NW, reflecting convergence between the Eurasian and African Plates.

## The North American-African Plate Boundary

This part of the Mid-Atlantic Ridge is cut by unusually many large offset fracture zones. North of 25°N all the fracture zones offset the ridge crest to the right, but south of 25° N almost all offsets are to the left. This shapes the ridge system into an arcuate structure, concave to the east, reflecting the original shape of the continents at the time of break-up. Major transform faults can be identified on the seismicity maps (Figures 8 and 9) by one or more of their seismic characteristics, i.e. east-west alignment of epicenters, offset in the ridge crest seismic zone, and fault plane solutions indicating strike-slip faulting in the transform sense. Thus left-lateral slip is demonstrated in the zones where the ridge axis is offset to the right, such as in the Oceanographer Fracture Zone (1 solution) and the Hayes Fracture Zone (1 solution). Right-lateral faulting, on the other hand, is shown in the Kane (3 solutions), 15° 20'(3 solutions), Vema (2 solutions) and Doldrums Fracture Zones (2 solutions). The last one is a multiple fracture zone, consisting of 3-4 transform faults.

All fault plane solutions obtained for earthquakes at or near the ridge crest show normal faulting, and where sufficient data are available the solutions have nonorthogonal nodal planes. For this reason the orientation of the fault planes and the stress axes cannot be determined with confidence. Yet it is clear that these are variable, even for closely spaced events. The two normal faulting events near 33°N (Figure 8), for example, have nearly identical epicenters, but the first motion pattern of the P waves is considerably different.

Only two fault plane solutions deviate from the general pattern established above; one in the Oceanographer Fracture Zone, the other in the Hayes Fracture Zone. The former (70 11) appears to have a large component of normal faulting. Reexamination of the seismograms showed that this earthquake is a complicated event, with the first motion of the main event obscured by a small foreshock on many records. This can hardly be considered a reliable solution. The other solution shows a significant component of reverse faulting in the Hayes Fracture Zone. Large scale vertical movements are indicated by the presence of transverse ridges in some of the major fracture

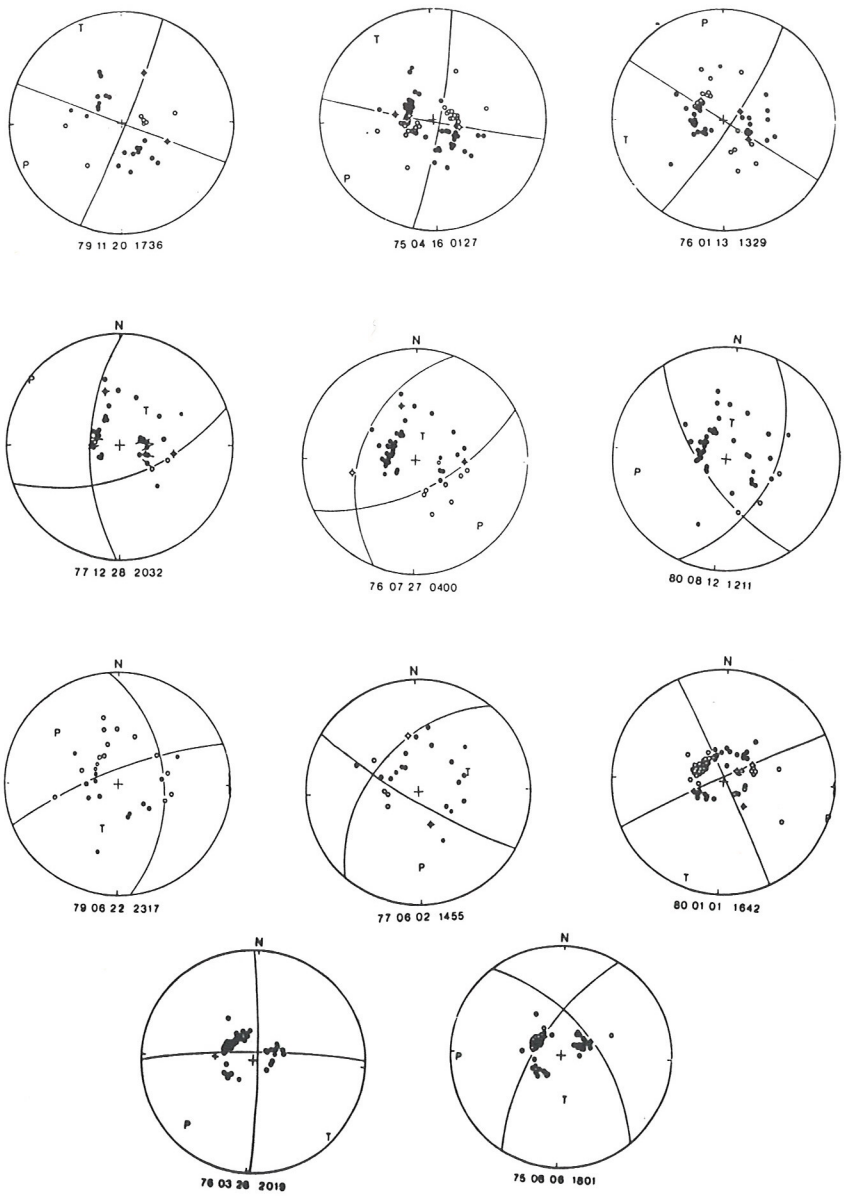


Fig. 10. Fault plane solutions shown on a stereographic projection of the lower hemisphere of the radiation field. Open circles are dilatational first motions of P-waves; compressional first motions are dots. Crosses indicate that the P-wave has a nodal character. S-wave polarization is shown with line segments. P and T are inferred axes of compression and tension, in the center of the dilatational and compressive fields of the focal sphere, respectively. Small symbols denote unreliable readings.

zones [Bonatti, 1978; Bonatti and Chermak, 1981; Bonatti et al., 1983] and seem to be an integral part of the tectonic regime of a transform fault. Occasional occurrence of reverse faulting events in fracture zones should therefore not be too surprising.

## Conclusions

The area studied here contains the part of the mid-oceanic ridge system that is most easily studied by seismological methods because of its favorable location with respect to the dense seismic

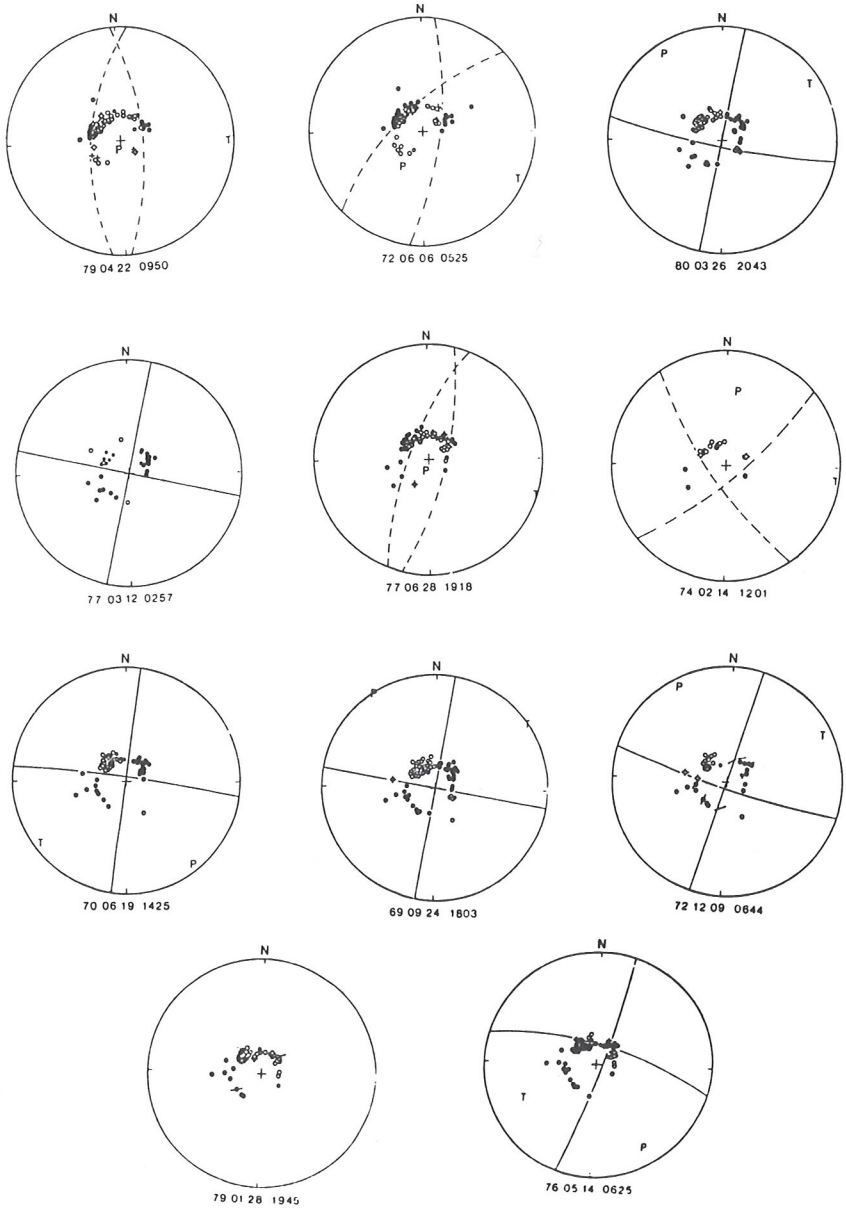


Fig. 10. (continued)

networks of Europe and N-America. It is here that we can hope to get the most complete picture of the faulting processes at mid-oceanic ridges by the study of earthquake focal mechanisms. The present compilation of fault plane solutions confirms the main results of Sykes [1967] that earthquakes in fracture zones are associated with transform faulting and that earthquakes along ridge axes are mainly associated with extensional tectonics. Thus nearly all fracture zone events, for which fault plane solutions have been obtained (35 of 37), were associated with transform faulting. For 25 out of 32 ridge crest events the fault plane solution had a large component of normal faulting. All the normal faulting events with sufficient focal sphere coverage have anomalous radiation pattern, i.e. orthogonal nodal planes cannot be found. Several explanations have been suggested for this phenomenon, but the one considered most likely is the interference of the surface reflected phases pP and sP with the direct P-wave. Fault plane solutions with large compo-

TABLE 1. Compilation of Fault Plane Solutions of North Atlantic and Arctic Earthquakes

| Date | | | Time | Epicenter | | $m_b$ | Poles of Nodal Planes | | P-axis | T-axis | O-axis | Data |
|---|---|---|---|---|---|---|---|---|---|---|---|---|
| Y | M | D | HM | N | W | | Tr/Pl | Tr/Pl | Tr/Pl | Tr/Pl | Tr/Pl | Source |
| 1969 | 04 | 07 | 2026 | 76.5 | -130.8 | 5.5 | 234/28 | 102/32(1) | 171/54 | 77/2 | 346/36 | 7(6,18) |
| 1964 | 08 | 25 | 1347 | 78.1 | -126.6 | 6.1 | 248/36 | 94/32(1) | 165/71 | 262/2 | 351/19 | 24 |
| 1970 | 04 | 23 | 0055 | 80.7 | -122.0 | 5.1 | 136/40 | 242/18 | 196/43 | 93/14 | 350/44 | 18 |
| 1975 | 02 | 26 | 0448 | 85.1 | -98.0 | 5.4 | 182/42 | 64/28 | 112/52 | 214/10 | 312/36 | 18 |
| 1975 | 03 | 02 | 1423 | 85.0 | -98.2 | 5.0 | 178/34 | 64/30 | 118/50 | 212/4 | 305/40 | 18 |
| 1968 | 06 | 08 | 0041 | 87.1 | -51.3 | 5.2 | 158/36 | 6/50 | 109/75 | 349/6 | 258/13 | 18 |
| 1964 | 07 | 31 | 2345 | 86.3 | -40.5 | 5.2 | 241/37 | 359/31 | 307/53 | 209/6 | 116/38 | 18 |
| 1967 | 03 | 14 | 0750 | 82.5 | -40.5 | 4.6 | 82/55 | 297/31 | 344/68 | 101/12 | 195/16 | 18 |
| 1968 | 04 | 07 | 0516 | 81.5 | 3.9 | 5.2 | 36/46 | 132/7 | 94/40 | 352/16 | 245/46 | 18 |
| 1972 | 11 | 19 | 2010 | 80.4 | 2.6 | 5.3 | 44/4 | 134/2 | 359/1 | 89/5 | 260/85 | 18 |
| 1972 | 11 | 25 | 2003 | 80.3 | 2.4 | 5.5 | 56/30 | 154/14 | 11/12 | 108/32 | 264/55 | 18 |
| 1967 | 11 | 23 | 1342 | 80.2 | 1.0 | 5.7 | 38/16 | 130/6 | 352/6 | 85/16 | 242/72 | 12 |
| 1967 | 10 | 18 | 0111 | 79.8 | -2.4 | 5.6 | 41/19 | 133/4 | 355/10 | 88/17 | 236/70 | 12 |
| 1970 | 10 | 26 | 2053 | 79.8 | -2.5 | 5.5 | 48/14 | 317/4 | 1/14 | 93/6 | 213/76 | 7(18) |
| 1971 | 11 | 26 | 2307 | 79.5 | 17.8 | 5.1 | 333/38 | 100/38 | 33/60 | 126/1 | 217/30 | 26 |
| 1976 | 01 | 18 | 0446 | 77.9 | -18.6 | 5.6 | 30/12 | 298/8 | 75/2 | 343/15 | 171/76 | 5(15,18) |
| 1970 | 10 | 21 | 0814 | 74.6 | -8.4 | 5.5 | 43/29 | 300/26 | 349/39 | 82/3 | 175/51 | 18 |
| 1968 | 01 | 03 | 0737 | 72.2 | -1.2 | 5.3 | 300/30 | 52/32 | 354/46 | 86/1 | 178/44 | 18 |
| 1971 | 05 | 31 | 0346 | 72,2 | -1.2 | 5.5 | 322/26 | 132/36(1) | 12/80 | 138/4 | 229/7 | 7(18) |
| 1975 | 01 | 20 | 1047 | 71.8 | -14.6 | 5.1 | 106/28 | 199/7 | 154/35 | 59/14 | 300/61 | 18 |
| 1971 | 03 | 23 | 0926 | 71.0 | 7.0 | 6.0 | 30/16 | 296/18 | 253/1 | 344/24 | 158/67 | 7(18) |
| 1979 | 11 | 20 | 1736 | 71.2 | 8.0 | 5.6 | 22/0 | 292/5 | 247/3 | 337/3 | 112/85 | 2 |
| 1970 | 02 | 22 | 2341 | 71.1 | 8.6 | 5.2 | 21/3 | 290/16 | 244/9 | 336/14 | 119/73 | 18 |
| 1972 | 09 | 08 | 1134 | 71.6 | 10.0 | 5.7 | 12/20 | 280/10 | 56/4 | 322/20 | 163/67 | 18 |
| 1975 | 04 | 16 | 0127 | 71.5 | 10.4 | 6.1 | 12/3 | 282/8 | 237/3 | 327/8 | 121/82 | 2(5,18) |
| 1974 | 03 | 22 | 1910 | 70.7 | 14.7 | 5.0 | 222/24 | 116/32 | 170/40 | 78/4 | 342/50 | 18 |
| 1969 | 05 | 05 | 2147 | 66.8 | 18.2 | 5.1 | 22/8 | 115/18 | 159/8 | 67/19 | 270/70 | 7 |
| 1963 | 03 | 28 | 0015 | 66.3 | 19.8 | 5.5 | 197/3 | 287/12 | 333/7 | 241/10 | 88/77 | 24(23,22) |
| 1976 | 01 | 13 | 1329 | 66.2 | 16.7 | 6.0 | 212/0 | 302/10 | 348/7 | 257/7 | 122/80 | 2(5,18) |
| 1974 | 06 | 12 | 1755 | 64.8 | 21.2 | 5.2 | 132/34 | 268/48 | 187/64 | 313/11 | 28/24 | 9 |
| 1974 | 07 | | | 64.8 | 21.4 | - | 0/45 | 180/45 | -/90 | 0/0 | 90/0 | 9,3 |
| 1977 | 12 | 28 | 2032 | 64.7 | 17.3 | 5.0 | 341/32 | 92/30 | 306/1 | 38/47 | 215/44 | 2 |
| 1976 | 07 | 27 | 0400 | 64.7 | 17.4 | 5.2 | 333/30 | 110/52 | 134/13 | 17/64 | 230/20 | 2 |
| 1980 | 08 | 12 | 1211 | 64.7 | 17.3 | 5.2 | 291/47 | 50/25 | 255/12 | 3/55 | 158/32 | 2 |
| 1979 | 06 | 22 | 2317 | 64.6 | 17.4 | 5.4 | 159/15 | 265/45 | 309/18 | 199/45 | 54/41 | 2 |
| 1967 | 07 | 27 | 0517 | 64.0 | 20.7 | 5.0 | 0/0 | 90/0 | 45/0 | 135/0 | -/90 | 29 |
| 1968 | 12 | 05 | 0944 | 63.9 | 21.7 | 5.5 | 357/0 | 267/15 | 221/9 | 313/10 | 87/75 | 29(18) |
| 1973 | 09 | 15 | 0145 | 63.9 | 22.2 | 5.3 | 180/12 | 271/2 | 226/10 | 134/8 | 9/78 | 8 |
| 1972 | 09 | | | 63.8 | 22.7 | - | 153/42 | 296/42 | 225/70 | 135/0 | 45/20 | 14 |
| 1977 | 06 | 02 | 1455 | 63.7 | 19.1 | 4.9 | 32/10 | 132/45 | 180/23 | 70/38 | 293/44 | 2 |
| 1969 | 09 | 20 | 0508 | 58.3 | 32.2 | 5.5 | (1) | | 172/72 | 278/5 | 9/15 | 8(20,11) |
| 1970 | 04 | 24 | 0123 | 55.7 | 35.0 | 5.3 | (1) | | -/90 | 293/0 | 13/0 | 27(8) |
| 1972 | 04 | 03 | 1852 | 54.3 | 35.1 | 5.3 | (1) | | -/90 | 95/0 | 5/0 | 27(8) |
| 1972 | 04 | 03 | 2036 | 54.3 | 35.1 | 5.1 | (1) | | -/90 | 95/0 | 5/0 | 27(8) |
| 1965 | 07 | 05 | 0831 | 52.9 | 34.2 | 5.7 | 16/10 | 107/8 | 331/1 | 61/12 | 235/77 | 25 |
| 1967 | 02 | 13 | 2414 | 52.8 | 34.1 | 5.5 | 10/0 | 100/6 | 146/4 | 56/4 | 280/84 | 8(19,13) |
| 1966 | 04 | 08 | 0552 | 52.7 | 33.3 | 5.2 | (12/0) | (102/0) | (147/0) | (57/0) | (-/90) | 8 |
| 1974 | 10 | 16 | 0545 | 52.6 | 32.1 | 5.8 | 5/2 | 95/0 | 320/1 | 50/1 | 185/88 | 13 |
| 1969 | 09 | 24 | 0358 | 52.5 | 31.9 | 5.1 | 4/0 | 94/0 | 139/0 | 49/0 | -/90 | 8 |
| 1964 | 08 | 26 | 0318 | 52.1 | 30.1 | 5.3 | 214/39 | 116/9 | 157/33 | 261/20 | 16/50 | 8 |
| 1970 | 09 | 18 | 1612 | 51.1 | 29.6 | 5.1 | 6/10 | 270/32 | 224/16 | 323/30 | 108/56 | 8 |
| 1973 | 01 | 05 | 0144 | 49.5 | 28.2 | 5.3 | 55/32 | 183/45 | 212/6 | 109/61 | 305/29 | 8 |
| 1972 | 11 | 07 | 1205 | 49.0 | 39.4 | 5.1 | 253/47 | 142/22 | 294/15 | 184/50 | 35/37 | 28 |
| 1965 | 09 | 29 | 2320 | 45.2 | 28.2 | 5.3 | 113/16 | (1) | (113/68) | (293/22) | (23/0) | 8(28) |
| 1964 | 09 | 17 | 1502 | 44.5 | 31.3 | 5.5 | 263/59 | 132/22 | 296/21 | 166/20 | 34/21 | 26(28) |
| 1964 | 09 | 18 | 1312 | 39.8 | 29.7 | 5.5 | 292/6 | 188/64 | 268/45 | 135/35 | 25/25 | 28 |
| 1973 | 11 | 23 | 1336 | 38.5 | 28.3 | 5.0 | 27/4 | 297/4 | 252/5 | 342/5 | 162/85 | 17 |
| 1980 | 01 | 01 | 1642 | 38.8 | 27.8 | 6.0 | 243/2 | 153/4 | 107/1 | 199/4 | 353/86 | 2(17) |
| 1964 | 09 | 06 | 1855 | 38.3 | 26.6 | 4.8 | 81/30 | 346/10 | 126/14 | 28/29 | 240/57 | 28 |
| 1966 | 07 | 04 | 1215 | 37.5 | 24.7 | 5.3 | 22/20 | 276/36 | 334/40 | 235/10 | 132/48 | 4(16) |
| 1966 | 07 | 05 | 0509 | 37.6 | 24.7 | 5.0 | 89/30 | 354/10 | 135/13 | 37/29 | 248/58 | 28 |
| 1975 | 05 | 26 | 0911 | 36.0 | 17.6 | 6.7 | 120/22 | 225/25 | 171/38 | 263/2 | 355/54 | 17 |
| 1975 | 03 | 08 | 0840 | 38.6 | 14.8 | 4.7 | 185/12 | 311/75 | 353/33 | 198/54 | 93/12 | 17 |
| 1970 | 12 | 30 | 2057 | 37.2 | 14.3 | 5.0 | 158/10 | 278/74 | 326/36 | 174/52 | 65/14 | 17 |
| 1969 | 07 | 26 | 1224 | 43.7 | 14.6 | 4.7 | 159/8 | 295/76 | 331/34 | 170/54 | 67/10 | 17 |
| 1969 | 09 | 06 | 1430 | 36.9 | 11.9 | 5.7 | 209/2 | 120/10 | 165/10 | 73/4 | 313/80 | 17(16,28) |

TABLE 1. (continued)

| Date | | | Time | Epicenter | | $m_b$ | Poles of Nodal Planes | | P-axis | T-axis | O-axis | Data |
|---|---|---|---|---|---|---|---|---|---|---|---|---|
| Y | M | D | HM | N | W | | Tr/Pl | Tr/Pl | Tr/Pl | Tr/Pl | Tr/Pl | Source |
| 1972 | 04 | 18 | 0551 | 36.4 | 11.1 | 4.7 | 196/12 | 292/22 | 335/6 | 242/25 | 77/64 | 17 |
| 1962 | 12 | 26 | 0858 | 39.3 | 10.6 | 5.0 | 344/19 | 85/24 | 126/3 | 33/32 | 240/58 | 17 |
| 1969 | 02 | 28 | 0240 | 36.0 | 10.6 | 7.3 | 142/40 | 0/46 | 340/4 | 78/72 | 249/18 | 17(16,10,28) |
| 1969 | 02 | 28 | 0425 | 36.2 | 10.5 | 5.7 | 142/30 | 0/54 | 337/12 | 100/68 | 243/18 | 17(16) |
| 1964 | 03 | 15 | 2230 | 36.2 | 7.6 | 6.2 | 335/10 | 206/74 | 165/34 | 320/54 | 66/12 | 28(4,16) |
| 1964 | 05 | 17 | 1926 | 35.2 | 35.9 | 5.5 | 176/6 | 267/16 | 219/16 | 311/7 | 64/73 | 24(28,30) |
| 1970 | 11 | 18 | 1223 | 35.1 | 35.7 | 5.3 | 233/30 | 123/30 | 181/45 | 88/1 | 358/45 | 28 |
| 1976 | 03 | 28 | 2019 | 33.8 | 38.6 | 5.5 | 177/8 | 268/5 | 224/10 | 131/3 | 30/80 | 2 |
| 1975 | 08 | 06 | 1801 | 33.8 | 39.3 | 5.4 | 229/34 | 120/26 | 267/4 | 173/46 | 359/45 | 2 |
| 1979 | 04 | 22 | 0950 | 33.0 | 39.7 | 5.7 | (1) | | 195/80 | 92/3 | 2/10 | 2 |
| 1972 | 06 | 06 | 0525 | 33.0 | 39.9 | 5.5 | (1) | | 212/51 | 117/3 | 24/40 | 2 |
| 1962 | 08 | 06 | 0135 | 32.0 | 40.8 | - | 196/40 | 319/33 | 263/57 | 166/4 | 73/33 | 24(21) |
| 1965 | 11 | 16 | 1524 | 31.0 | 41.5 | 6.0 | (1) | | 193/60 | 283/0 | 13/30 | 24(30) |
| 1963 | 05 | 19 | 2135 | 23.8 | 46.0 | 5.8 | 13/0 | 284/3 | 329/2 | 239/2 | 103/87 | 24(22) |
| 1980 | 03 | 26 | 2043 | 23.9 | 45.6 | 5.9 | 11/8 | 101/0 | 325/6 | 56/6 | 191/82 | 2 |
| 1977 | 03 | 12 | 0257 | 23.8 | 45.2 | 5.4 | (13/0) | (103/0) | (328/0) | (58/0) | (-/90) | 2 |
| 1977 | 06 | 28 | 1918 | 22.6 | 45.1 | 5.8 | (1) | | 202/79 | 108/1 | 18/11 | 2 |
| 1974 | 02 | 14 | 1201 | 22.0 | 44.3 | 5.4 | 54/18 | 320/15 | 7/24 | 97/1 | 191/68 | 2 |
| 1965 | 06 | 02 | 2340 | 15.9 | 46.6 | 5.7 | (1) | | 158/64 | 269/9 | 3/24 | 25(30) |
| 1970 | 06 | 19 | 1425 | 15.4 | 46.0 | 5.5 | 188/5 | 98/0 | 143/4 | 233/4 | 8/85 | 2(30) |
| 1969 | 09 | 24 | 1803 | 15.2 | 45.8 | 5.7 | 10/0 | 100/0 | 315/0 | 55/0 | -/90 | 2 |
| 1972 | 12 | 09 | 0644 | 15.2 | 45.2 | 5.6 | 16/7 | 106/0 | 330/4 | 61/4 | 196/83 | 2 |
| 1979 | 01 | 28 | 1945 | 11.9 | 43.7 | 5.8 | | | (-/90) | (90/0) | (0/0) | 2 |
| 1976 | 05 | 14 | 0625 | 10.8 | 43.5 | 5.6 | 195/22 | 287/6 | 149/10 | 243/20 | 33/67 | 2 |
| 1962 | 03 | 17 | 2047 | 10.9 | 43.2 | - | 180/4 | 270/6 | 315/0 | 225/7 | 53/83 | 24(23) |
| 1963 | 11 | 17 | 0048 | 7.6 | 37.4 | 5.8 | 188/4 | 98/0 | 143/2 | 233/2 | 8/86 | 24(22) |
| 1963 | 08 | 03 | 1021 | 7.7 | 35.8 | 6.0 | 10/11 | 100/0 | 325/8 | 55/8 | 190/79 | 24(22) |
| 1965 | 08 | 16 | 1236 | -0.5 | 20.0 | 6.1 | 354/16 | 85/7 | 316/5 | 41/18 | 199/72 | 25 |
| 1965 | 11 | 15 | 1118 | -0.2 | 18.7 | 5.6 | 357/20 | 88/6 | 311/9 | 44/18 | 197/70 | 24 |

nents of reverse faulting were found at the ridge axis in two areas; in the Bardarbunga central volcano in Iceland and near 50° N. Several mechanisms may be found to explain reverse faulting at a divergent plate boundary, but the one favoured here is brittle failure of the crust above a deflating, localized magma chamber.

## Appendix 1. New and Revised Fault Plane Solutions

Focal sphere plots of P-wave first motions and S-wave polarizations are shown in Fig. 10. Nodal planes, T- and P-axes are shown when they could be determined with reasonable accuracy. For normal faulting earthquakes the apparent nodal planes are probably not planar, although they have been approximated by planes.

79 11 20 1736h, Jan Mayen Fracture Zone. This is a reasonably well determined strike-slip solution in spite of relatively high microseismic disturbance at N-American stations. The sense of motion is left-lateral if the slip is along the fracture zone.

75 04 16 0127h, Jan Mayen Fracture Zone. This is a well constrained strike-slip solution, left-lateral if slip occurs along the fracture zone.

76 01 13 1329h, Tjornes Fracture Zone. This is a well constrained strike-slip solution, right-lateral if slip occurs along the Grímsey seismic lineament.

77 12 28 2032h, Bárdarbunga Central Volcano. This is clearly a reverse faulting solution. One nodal plane (strike 71°) is well determined, the other s determined mostly by the constraint of orthogonality. Assuming shallower focus would allow more freedom in strike, e.g. T-axis could be closer to vertical, which fits better to the S-wave observations.

76 07 27 0400h, Bárdarbunga Central Volcano. This clearly is a reverse faulting solution. One nodal plane (strike 64°) is well constrained, the dip of the other one mainly found by the constraint of orthogonality, its strike is affected by the assumed depth of focus and the local velocity model.

80 08 12 1211h, Bárdarbunga Central Volcano. The solution has a large component of reverse faulting. One nodal plane (strike 21°) is well determined, the other is found by the constraint of orthogonality.

79 06 22 2317h, Bárdarbunga Central Volcano. The solution has a significant reverse faulting component, but the attitude of the nodal planes is highly dependent on the assumption of orthogonality.

77 06 02 1455h, Katla Central Volcano. The solution indicates a mixture of strike-slip and

reverse faulting. No solution free of inconsistencies could be found. The preferred solution is a compromise.

80 01 01 1642h, Azores. A pure strike-slip solution fits the first motion data best. The sense of motion is left-lateral, if slip is along the plane striking 153° as shown by aftershocks.

76 03 28 2019h, Hayes Fracture Zone. The solution shows strike-slip faulting, left-lateral motion if slip along the fracture zone is assumed.

75 08 08 1801h, Hayes Fracture Zone. This solution has a significant component of reverse faulting. One nodal plane (strike 30°) is reasonably well constrained by the N.-American stations. The other plane is determined by one nodal reading and the constraint of orthogonality.

79 04 22 0950h, Ridge axis near 33° N. This is a normal faulting solution with nonorthogonal nodal surfaces. Many of the dilatational first motions have a nodal character.

72 06 06 0525h, Ridge axis near 33° N. This is a normal faulting solution with nonorthogonal nodal surfaces. In spite of nearly identical epicenter to the previous event, the first motion pattern of the two earthquakes is different.

80 03 26 2043h, Kane Fracture Zone. This is a well controlled strike-slip solution, right-lateral motion if slip occurs along the fracture zone.

77 03 12 0257h, Kane Fracture Zone. A strike-slip solution with right-lateral slip along the fracture zone fits the data well. The solution is highly nonunique, however. The strike of the nodal planes can be varied as much as 10°, and a thrust mechanism is possible with only minor inconsistencies.

77 06 28 1918h, Ridge axis near 22.6° N. This event is part of a large earthquake swarm. Three events were analyzed; at 1538, 1618 and 1918h. Judged from the long period body and surface waves, all the events had similar faulting mechanism. Small differences were seen in the short period wave forms. The best solution was obtained for the 1918 event. It is a normal faulting solution with non-orthogonal nodal surfaces. Most dilatational first motions have a nodal character.

74 02 14 1201h, Intraplate event. This solution is not well constrained, but is probably of the strike-slip type. The earthquake appears to be a typical intraplate event with small surface waves, and impulsive short-period P-waves. Most of the first motions are read from short-period records.

70 06 19 1425h, 15° 20' Fracture Zone. This is a strike-slip solution, right-lateral motion if slip is along the fracture zone. Because of the concentration of stations near the center of the plot, dips of the nodal planes are well determined, but the strikes are not. A nodal plane striking parallel to the fracture zone fits the data well, but the strike could be varied as much as 10°.

69 09 24 1803h, 15° 20' Fracture Zone. This is a well controlled strike-slip solution, right-lateral motion if slip is along the fracture zone.

72 12 09 1644h, 15° 20' Fracture Zone. This is a strike-slip solution similar to the two previous ones. Nodal plane of the preferred solution has a strike of 106°, but is not well constrained. The strike can be varied within a 23° angle without adding inconsistencies.

79 01 28 1945h, Ridge axis near 12° N. This event is the largest in a swarm that lasted at least 14 hours. The wave form and pattern of first motions indicate normal faulting, but the attitude of the nodal surfaces cannot be determined. The S-wave polarizations indicate a nearly vertical P-axis.

76 05 14 0625h, Vema Fracture Zone. This is a strike-slip solution with a small component of reverse faulting. The sense of motion is consistent with transform faulting even though the preferred nodal plane strikes slightly oblique to the fracture zone and dips to the north. This event is located near the ridge - fracture zone intersection.

## Appendix 2. Compilation of Fault Plane Solutions

Earthquakes for which fault plane solutions have been determined are listed in geographical order in Table 1, along with parameters of the solutions. Reference to the data source is given in the last column by a number, alternate solutions or reference to further studies are given in parentheses as follows:

1. Nonorthogonal nodal planes
2. This paper
3. Average solution for a number of small earthquakes, determined with a dense, local array
4. Banghar and Sykes, 1969
5. Bungum, 1978
6. Chapman and Solomon, 1976
7. Conant, 1972
8. Einarsson, 1979
9. Einarsson et al., 1977
10. Fukao, 1973
11. Hart, 1978
12. Horsfield and Maton, 1970
13. Kanamori and Stewart, 1976
14. Klein et al., 1977
15. Mitchell et al., 1977
16. McKenzie, 1972
17. Moreira, 1982
18. Savostin and Karasik, 1981
19. Solomon, 1973
20. Solomon and Julian, 1974
21. Stauder and Bollinger, 1964
22. Stauder and Bollinger, 1966
23. Stefánsson, 1966
24. Sykes, 1967
25. Sykes, 1970
26. Sykes and Sbar, 1974
27. Tréhu et al., 1981
28. Udias et al., 1976
29. Ward, 1971
30. Weidner and Aki, 1973

Note added in proof. Since the acceptance of this paper for publication, significant progress has been made in the study of source mechanisms of mid-oceanic earthquakes. A few remarks in the paper may therefore seem out of place.

Acknowledgements. Financial contribution was obtained from the Icelandic Science Fund for this work. The WWSSN film chips library at Lamont-Doherty Geological Observatory was used extensively; the help and hospitality of Drs. R. Bilham and D. Simpson is gratefully acknowledged. Sigfús Johnsen, Sigurdur E. Pálsson and Bryndís Brandsdóttir helped with computing and plotting, Kristín Pálsdóttir typed the manuscript.

References

Banghar, A.R., and L.R. Sykes, Focal mechanisms of earthquakes in the Indian Ocean and adjacent regions, J. Geophys. Res., 74, 632-649, 1969.

Beblo, M., and A. Björnsson, A model of electrical resistivity beneath NE-Iceland, correlation with temperature, J. Geophys., 47, 184-190, 1980.

Björnsson, A., K. Saemundsson, P. Einarsson, E. Tryggvason, and K. Gronvold, Current rifting episode in north Iceland, Nature, 266, 318-323, 1977.

Bonatti, E., Vertical tectonism in oceanic fracture zones, Earth Planet. Sci. Letters, 37, 369-379, 1978.

Bonatti, E., and A. Chermak, Formerly emerging crustal blocks in the equatorial Atlantic, Tectonophysics, 72, 165-180, 1981.

Bonatti, E., R. Sartori, and A. Boersma, Vertical crustal movements at the Vema Fracture Zone in the Atlantic: Evidence from dredged limestones, Tectonophysics, 91, 213-232, 1983.

Bungum, H., Reanalyzation of three focal mechanism solutions for earthquakes from Jan Mayen, Iceland and Svalbard, Tectonophysics, 51, T15-T16, 1978.

Bungum, H., B.J. Mitchell, and Y. Kristoffersen, Concentrated earthquake zones in Svalbard, Tectonophysics, 82, 175-188, 1982.

Bungum, H., and E.S. Husebye, Seismicity of the Norwegian Sea: The Jan Mayen Fracture Zone, Tectonophysics, 40, 351-360, 1977.

Chapman, M.E., and S.C. Solomon, North American-Eurasian plate boundary in Northeast Asia, J. Geophys. Res., 81, 921-930, 1976.

Conant, D.A., Six new focal mechanism solutions for the Arctic and a center of rotation for plate movements, M.A. Thesis, Columbia University, New York, 1972.

Gebrande, H., H. Miller, and P. Einarsson, Seismic structure of Iceland along RRISP-Profile I, J. Geophys., 47, 239-249, 1980.

Einarsson, P. Relative location of earthquakes within the Tjörnes Fracture Zone, Soc. Sci. Isl., Greinar V, 45-60, 1976.

Einarsson, P. Seismicity and earthquake focal mechanisms along the mid-Atlantic plate boundary between Iceland and the Azores, Tectonophysics, 55, 127-153, 1979.

Einarsson, P., Seismicity along the eastern margin of the North American Plate. Manuscript, to be published by the Geol. Soc. America, 1985.

Einarsson, P., and J. Eiríksson, Earthquake fractures in the districts Land and Rangárvellir in the South Iceland Seismic Zone, Jökull, 32, 113-120, 1982.

Einarsson, P., S. Björnsson, G. Foulger, R. Stefánsson, and p. Skaftadottir, Seismicity pattern in the South Iceland seismic zone, Earthquake Prediction - An International Review, Maurice Ewing Series 4, Am. Geophys. Union, p. 141-151, 1981.

Einarsson, P., F.W. Klein, and S. Björnsson, The Borgarfjördur earthquakes of 1974 in West Iceland, Bull. Seism. Soc. Am., 67, 187-208, 1977.

Forsyth, D., and H. Rowlett, Microearthquakes and recent faulting at the intersection of the Vema fracture zone and the Mid-Atlantic Ridge (abstract), EOS Trans. AGU, 60, 376, 1979.

Foulger, G.R., The Hengill geothermal area: Seismological studies 1978-1984, Science Institute, Univ. Iceland, Rep. RH-07-84, 96 pp., 1984.

Fukao, Y., Thrust faulting at a lithospheric plate boundary, the Portugal earthquake of 1969, Earth Planet. Sci. Lett., 18, 205-216, 1973.

Hart, R.S., Body wave observations from the September, 1969, North Atlantic Ridge earthquake (abstract), EOS, Trans. Amer. Geophys. Union, 59, 326, 1978.

Hirn, A., H. Haessler, P. Hoang Trong, G. Wittlinger, and L.A. Mendes Victor, Aftershock sequence of the January 1st, 1980, earthquake and present-day tectonics in the Azores, Geophys. Res. Lett., 7, 501-504, 1980.

Horsfield, W.T., and P.I. Maton, Transform faulting along the De Geer line, Nature, 226, 256-257, 1970.

Johnson, G.L., and P.R. Vogt, Mid-Atlantic ridge from 47° to 51° N, Geol. Soc. Amer. Bull., 84, 3443-3462, 1973.

Julian, B.R., Evidence for dyke intrusion earthquake mechanisms near Long Valley Caldera, California, Nature, 303, 323-325, 1983.

Kanamori, H., and G.S. Stewart, Mode of strain release along the Gibbs fracture zone, mid-Atlantic ridge, Phys. Earth Planet. Interiors, 11, 312-331, 1976.

Kawasaki, I., and T. Tanimoto, Radiation patterns of body waves due to the seismic dislocation occurring in an anisotropic source medium, Bull. Seismol. Soc. Amer., 71, 37-50, 1981.

Klein, F.W., P. Einarsson, and M. Wyss, Microearthquakes on the mid-Atlantic plate boundary on the Reykjanes Peninsula in Iceland, J. Geophys. Res., 78, 5084-5099, 1973.

Klein, F.W., P. Einarsson, and M. Wyss, The Reykjanes Peninsula, Iceland, earthquake swarm

of September 1972 and its tectonic significance, J. Geophys. Res., 82, 865-888, 1977.
McKenzie, D., Active tectonics of the Mediterranean region, Geophys. J. R. Astr. Soc., 30, 109-185, 1972.
Mitchell, B.J., J.E. Zollweg, J.J. Kohsmann, C.-C. Cheng, and E.J. Hang, Intraplate earthquakes in the Svalbard archipelago, J. Geophys. Res., 84, 5620-5626, 1979.
Moreira, V., Seismotectonics of mainland Portugal and its adjacent region in the Atlantic (in Portugese, with English abstract), 29pp., Lisboa 1982.
Robson, G.R., K.G. Barr, and L.C. Luna, Extension failure: an earthquake mechanism, Nature, 218, 28-32, 1968.
Savostin, L.A., and A.M. Karasik, Recent plate tectonics of the Arctic Basin and of northeastern Asia, Tectonophysics, 74, 111-145, 1981.
Searle, R., The active part of Charlie-Gibbs fracture zone: A study using sonar and other geophysical techniques, J. Geophys. Res., 86, 243-262, 1981.
Sigvaldason, G.E., S. Steinthorsson, N. Óskarsson, and P. Imsland, Compositional variation in recent Icelandic tholeiites and the Kverkfjöll hot spot, Nature, 251, 579-582, 1974.
Solomon, S.C., Shear-wave attenuation and melting beneath the mid-Atlantic ridge, J. Geophys. Res., 78, 6044-6059, 1973.
Solomon, S.C., and B.R. Julian, Seismic constraints on ocean-ridge mantle structure: anomalous fault-plane solutions from first motions, Geophys. J. R. Astr. Soc., 38, 265-285, 1974.
Stauder, W., and G.A. Bollinger, The S-wave project for focal mechanism studies - earthquakes of 1962, Bull. Seismol. Soc. Am., 54, 2199-2208, 1964.
Stauder, W., and G.A. Bollinger, The S-wave project for focal mechanism studies, earthquakes of 1963, Bull. Seismol. Soc. Am., 56, 1362-1371, 1966.
Stefánsson, R., Methods of focal mechanism with application to two Atlantic earthquakes, Tectonophysics, 3, 209-243, 1966.
Sykes, L.R., Mechanism of earthquakes and nature of faulting on the mid-ocean ridges, J. Geophys. Res., 72, 2131-2153, 1967.
Sykes, L.R., Focal mechanism solutions for earthquakes along the world rift system, Bull. Seismol. Soc. Am., 60, 1749-1752, 1970.
Sykes, L.R., and M.L. Sbar, Focal mechanism solutions of intraplate earthquakes and stresses in the lithosphere; in: Geodynamics of Iceland and the North Atlantic Area (L. Kristjánsson ed.), D. Reidel Publishing Co., Dordrecht - Holland / Boston - USA, 1974.
Tams, E., Erdbeben im Gebiet der Nordenstkiöld See, Gerlands Beitr. z. Geophysik, 17, 325-331, 1927.
Trêhu, A.M., J.L. Nábělek, and S.C. Solomon, Source characterization of two Reykjanes Ridge earthquakes: Surface waves and moment tensors; P waveforms and non-orthogonal nodal planes, J. Geophys. Res., 86, 1701-1724, 1981.
Udias, A., A. Lopez Arroyo, and J. Mezcua, Seismotectonics of the Azores-Alboran region, Tectonophysics, 31, 259-289, 1976.
Vogt, P.R., Long wavelength gravity anomalies and intraplate seismicity, Earth Planet. Sci. Lett., 37, 465-475, 1978.
Ward, P.L., New interpretation of the geology of Iceland, Geol. Soc. Am. Bull., 82, 2991-3012, 1971.
Weidner, D.J., and K. Aki, Focal depth and mechanism of mid-ocean ridge earthquakes, J. Geophys. Res., 78, 1818-1831, 1973.
Whitmarsh, R.B., and A.S. Laughton, The fault pattern of a slow-spreading ridge near a fracture zone, Nature, 258, 509-510, 1975.